

Flipping photons backward: reversed Cherenkov radiation

Charged particles moving faster than light in a medium produce Cherenkov radiation. In traditional, positive index-of-refraction materials this radiation travels forward. Metamaterials, with negative indices of refraction, flip the radiation backward. This readily separates it from the particles, providing higher flexibility in photon manipulation and is useful for particle identification and counting. Here we review recent advances in reversed Cherenkov radiation research, including the first demonstration of backward emission. We also discuss the potential for developing new types of devices, such as ones that pierce invisibility cloaks.

Hongsheng Chen^{1,2} and Min Chen³

¹The Electromagnetics Academy at Zhejiang University, Zhejiang University, Hangzhou, 310027, China.

²Research Laboratory of Electronics, Massachusetts Institute of Technology, Cambridge, Massachusetts 02139, USA.

³Department of Physics, Massachusetts Institute of Technology, Cambridge, Massachusetts 02139, USA.

E-mail: hansomchen@zju.edu.cn; chenm@mit.edu.

Although the speed of light, or more precisely its phase velocity, is the ultimate velocity in a vacuum, it can be exceeded by particles in other media, such as water. When a charged particle travels through a dielectric medium at a speed greater than the phase velocity of light in that medium, electromagnetic radiation, or photons, are emitted as a Cherenkov cone. The blue glow seen in the water in nuclear reactors is an example of this. This phenomenon, known as Cherenkov radiation, was first observed by Cherenkov¹ and theoretically interpreted by Tamm and Frank². Since the energy and angle of the emission depend on the speed of the charged particles, the radiation can be used to detect and count those particles. Such devices, called Cherenkov counters, have made possible many prominent discoveries in nuclear and particle physics, including that of the antiproton³ and

the *J* particle⁴. Today Cherenkov radiation has been, and is being, widely used in experiments for identifying fast particles, measuring the intensity of reactions, detecting labeled biomolecules, and determining the source and intensity of cosmic rays.

Because Cherenkov waves are only emitted if a particle is traveling faster than the speed of light in a medium, Cherenkov radiation only arises from high-energy particles. Also, in a conventional dielectric medium, the emitted radiation travels in the same direction as the particles and forms an expanding cone. Consequently, the charged particles will interfere with the detection of those photons. All of these problems could be solved if the radiation and particles moved in opposite directions. This is now possible, thanks to recently developed metamaterials that offer some novel electromagnetic properties

not found in nature⁵⁻²⁰. In particular, metamaterials offer reversed Cherenkov radiation, a phenomenon in which the photon and charged particle naturally separate in opposite directions so that their physical interference is minimized. Therefore, the influence of the noise of high-energy particles on useful information can be suppressed and the Cherenkov detector is shielded from radiation damage.

With regard to Cherenkov radiation, of particular interest is that a properly designed metamaterial can be a left-handed or negative-refractive-index medium. That is, unlike all known natural mediums, a suitably engineered metamaterial can simultaneously have negative real parts of both permittivity ϵ and permeability μ . These parameters, like the associated refractive index, have both real and imaginary components. In a left-handed medium, the electric field vector E , the magnetic field vector H , and the wave vector k form a left-handed triad, hence the name left-handed material²¹. This is the mirror image of conventional mediums, which are right-handed.

This difference impacts wave propagation. In contrast to a conventional medium, the phase propagation direction represented by the wave vector is opposite to the energy flow in a left-handed medium²¹, due to the negative real part of its refractive index. In other words, the wave undergoes a negative phase change while propagating forward in a left-handed medium. This characteristic leads to a backward emitted Cherenkov wave, which can be easily separated from the high-energy particles that produce it. Such a medium can be constructed out of artificial resonant elements whose sizes and spacings are much smaller than the wavelength of interest. These artificial elements play roles similar to that of atoms or molecules. An appropriate collection of these components produces a macroscopic electromagnetic response characterized by negative permittivity and negative permeability. Suitable left-handed metamaterials will allow us to exploit some exotic phenomena associated with Cherenkov radiation and open a new window of novel applications in high-energy physics, astrophysics, biology, and elsewhere.

Here we provide an overview of the basis for reversed Cherenkov radiation, examine how to achieve it, review results demonstrating it, and explore applications of metamaterials in it. We conclude by highlighting the practical potential of this field and the challenging work that remains to be solved in order to realize that potential.

Preserving time's arrow

Understanding why a left-handed material flips the direction of Cherenkov radiation requires understanding the origin of that radiation. Fundamentally, it is a shockwave, the photonic equivalent of a fast boat's wake or the supersonic boom of a jet airplane. This photonic shockwave, or Cherenkov radiation, is created by a fast-moving charged particle as it barrels through a medium. Knowing this and something of the nature of left-handed metamaterials helps explain why there is neither a causality nor energy-momentum conservation paradox with backward Cherenkov radiation.

In a conventional, right-handed material, Cherenkov radiation possesses three key characteristics: 1) it appears only if the speed of the charged particle is greater than the speed of light in the medium, 2) the constant phase front of the radiated wave forms a cone and propagates forward, and 3) the polarization of the electric field vector lies in the plane determined by the velocity vector of charge and the direction vector of the power radiation. This last characteristic means that the radiation exhibits a transverse magnetic field (TM), which has implications for the metamaterial attributes required to reverse the radiation.

Fig. 1a illustrates the physical origin of Cherenkov radiation. The figure shows the E_z field of the wave radiated from a charged particle moving with a speed $v > c/n$ along the z -axis, where c is the speed of light in vacuum and n is the real part of the medium's refractive index. The particle's movement generates a forward Cherenkov radiation cone in a conventional material with a positive index of refraction. At time t_0 , the particle arrives at position 0 and drives the medium to radiate a spherical wave outward. A short time later (Δt), the particle has moved a distance of $v\Delta t$. During that time, the phase front of the radiated wave represented by the dashed lines in the figure has traveled a distance of $c\Delta t/n$. A shock wave is formed beside the particle with the group wave front coincident with the phase wave front. Both are perpendicular to the energy flux, represented by the Poynting vector. The angle between the direction of energy flow and the particle velocity is θ , which is determined by the particle's speed and the medium's refractive index by $\cos^{-1}[c/(nv)]$. The direction of the shock wave therefore forms a forward Cherenkov radiation cone with an angle of 2θ .

Fig. 1b shows the corresponding Cherenkov radiation in a left-handed medium with negative real part of the refractive index. As the particle travels along the z direction, the emitted wave has the energy flowing outward (blue arrows) in a cone with angle, $\theta = \cos^{-1}[c/(nv)]$. For $n < -1$ the angle is obtuse or backward pointing. The phase propagation represented by the wave vector (red arrows) is opposite the energy flow direction. As can be seen by the dashed lines in the figure, the phase fronts converge towards the path of the particle as time passes in what seems to be a violation of causality. This apparent paradox in the relationship between cause and effect is resolved because energy is carried by the group, and not the phase, velocity.

A left-handed medium is dispersive and so has a wavelength dependent response to radiation. In other words, its group and phase velocity are different. Thus, while the particle in Fig. 1b moves a distance of $v\Delta t$ the phase front travels a distance of $c\Delta t/n$ and the energy travels a distance of $c\Delta t/n_g$, where c/n and c/n_g are the phase and group velocities respectively. In this case, the group wave front is not perpendicular to the group velocity (energy direction). The cone angle of the group wave front, Φ , is $180^\circ - \tan^{-1}\{[(n/n_g)\sin\theta \cos\theta]/[1 - (n/n_g)\cos^2\theta]\}$. Consequently, the group wave front arising from the group propagation is no longer perpendicular to the Poynting vector. The shock wave is always behind

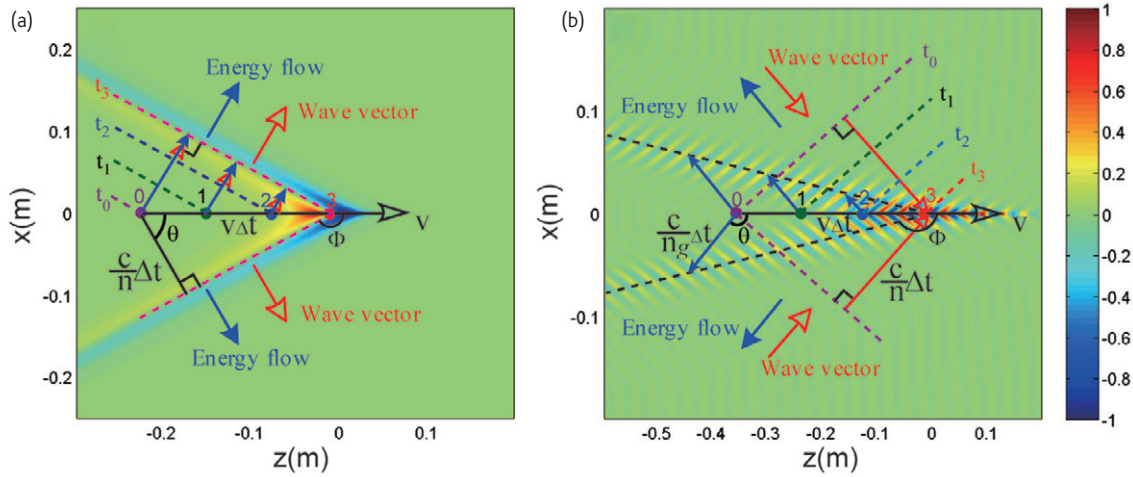


Fig. 1 E_z field of a photonic shockwave in a (a) conventional and (b) left-handed medium. Note that the energy flow is parallel to the wave vector in the conventional case and opposite for the left-handed case. (a) In a conventional medium with a real part of the refractive index $n=2$ and a charged particle with a velocity 99% of the speed of light in a vacuum, or $v = 0.99c$, the Cherenkov radiation forms a cone with $\theta = 60^\circ$. (b) Reversed Cherenkov radiation in a left-handed medium, with a fast moving charged particle with $v = 0.99c$. The energy flow forms a cone with an angle of $\theta = \cos^{-1}[c/(nv)] \approx 115^\circ$. The phase wave front forms a cone with an angle of $\Phi = 172.6^\circ$, where Φ satisfies the following equation $\tan(180^\circ - \Phi) = [(n/n_g)\sin\theta \cos\theta]/[1 - (n/n_g)\cos^2\theta]$. Both angles are related to

the relative permittivity and permeability of the medium. The relative permittivity follows a Drude dispersive model $\epsilon_r = 1 - \frac{\omega_{ep}^2}{\omega^2 + i\omega\gamma_e}$ with $f_{ep} = (2\pi)^{-1}\omega_{ep}^{-1} = 20$ GHz and $\gamma_e = 0.001\omega_{ep}$, and the relative permeability follows a Lorentz dispersive model $\mu_r = 1 - \frac{\omega_{mp}^2}{\omega^2 - \omega_0^2 + i\omega\gamma_m}$ with $f_{mp} = (2\pi)^{-1}\omega_{mp}^{-1} = 10$ GHz, $f_0 = (2\pi)^{-1}\omega_0^{-1} = 4$ GHz, and $\gamma_m = 0.002\omega_{mp}$. A window function $W(f) = \exp\left[-\frac{(f-f_c)^2}{2\sigma^2}\right]$ with $f_c = 8$ GHz and $\sigma = 0.5$ GHz is used to observe the Cherenkov radiation around the centre frequency of f_c . The phase refractive index at $f_c = 8$ GHz is $n = c/(\omega/k) = -\sqrt{\mu_r\epsilon_r} = -2.385$, and the group refractive index is $n_g = c/(d\omega/dk) = 6.569$.

the moving particle. Thus, the backward cone formed by the group wave front obeys causality.

Conserving energy and momentum

With time's arrow intact, another apparent paradox needs to be resolved. On first glance, it seems that reversed Cherenkov radiation violates energy-momentum conservation, with particles appearing to gain both momentum and energy. However, closer inspection shows that here too there is no problem.

A charged particle loses energy in emitting Cherenkov radiation and, therefore, slows down. The popular simple definition of the time averaged wave momentum density is $\langle G \rangle = \frac{1}{2}\text{Re}(\epsilon E \times \mu^* H^*)$. The term in parenthesis is known as the Minkowski momentum²²⁻²⁴. However, this definition no longer holds in a left-handed medium; this is a good thing, because if it did backward Cherenkov radiation would not conserve energy and momentum. To see why, consider the simple case of an isotropic left handed medium with appropriate ϵ and μ . The simple definition leads to the wave momentum in the same backward direction as the energy flow defined by the Poynting vector since the real parts of both ϵ and μ are negative. In order to conserve momentum, the charged particle must gain momentum and thus also energy, violating the conservation of energy²⁵.

The correct definition of $\langle G \rangle$ has been addressed in²⁶. If loss is negligible, then the proper formulation in a dispersive left-handed

medium, $\langle G \rangle = \frac{1}{2}\text{Re} \{ \epsilon E \times \mu^* H^* + \frac{1}{2} k[\partial\epsilon/\partial\omega] E \cdot E^* + (\partial\mu/\partial\omega) H \cdot H^* \}$, is the simple definition plus material dispersion terms related to the electric and magnetic fields. This momentum density vector can be shown to be equal to the number of photons per unit volume times $\hbar k$, where \hbar is the reduced Planck constant, in agreement with its definition in quantum physics^{21,25}. The time averaged Poynting vector $\langle S \rangle = \langle E \times H^* \rangle$ is opposite to the wave vector (see Box 1 for a discussion of this for a particular case), representing a backward propagating wave. The wave momentum is therefore in the forward direction, and the charge particle loses momentum and also energy as it travels through the medium. Momentum and energy are thus both conserved.

In an isotropic left-handed medium for which loss cannot be neglected, the momentum density $\langle G \rangle$ may be parallel to the energy flow²⁷. This is because the material dispersion terms in the expression of $\langle G \rangle$ become minor compared with the first term represented by Minkowski momentum. However, momentum is still conserved because a recoiled force opposed by the medium will be raised as the wave attenuates in the lossy medium²⁷.

Metamaterial design for reversed Cherenkov radiation

Realizing reversed Cherenkov radiation requires designing a suitable isotropic left-handed medium. Most of the previously designed left-handed materials will not work, as shown by the following.

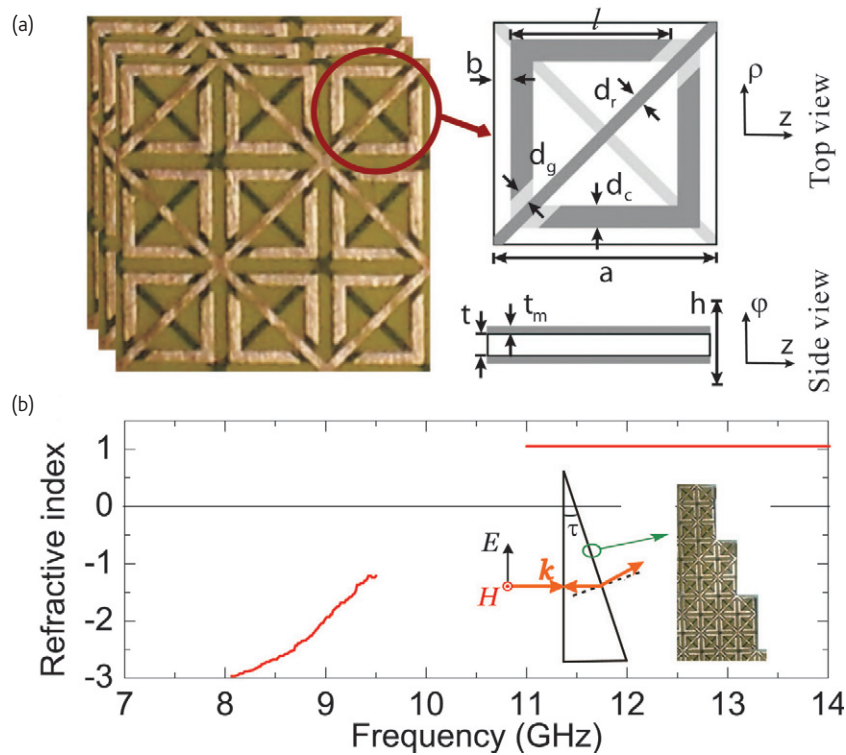


Fig. 2 (a) Configuration of the metamaterial for reversed Cherenkov radiation. (b) The measured real refractive index of the metamaterial, which is negative for frequencies between 8.1 and 9.5 GHz, for transverse magnetic polarized field incidence (the H indicating the magnetic field is perpendicular to the plane of the page). Reprinted figure with permission from³⁴. © 2009 by the American Physical Society.

The magnetic (μ) and electric (ϵ) tensors in general are 3×3 complex matrices. For the simple case of a charged particle moving and accelerated in the z -direction in a cylindrical coordinate system, the magnetic field is non-zero only along the φ direction and the electric field is non-zero only along the ρ and the z directions. Due to this symmetry, the only relevant components are along φ for the magnetic field and the other two orthogonal components for the electric field.

Previous metamaterial designs were mostly for electromagnetic waves with out-of-plane electric fields^{6,15-17,28-32}. Thus they are not suitable for testing reversed Cherenkov radiation, which requires a transverse magnetic field. With this in mind, a new type of left-handed metamaterial has recently been experimentally fabricated for the detection of Cherenkov radiation^{33,34}. An image is shown in Fig. 2a. The metamaterial is composed of many substrate layers repeated along the φ direction, with each layer consisting of split-ring resonators and metal wires. In each layer, orthogonal copper wires are printed on both sides of the thin dielectric sheet. They provide isotropic negative permittivity in the ρz plane, while the two L-shaped metal strips on the top side couple with the two on the bottom side to form an equivalent inductor/capacitor resonator. These supply a negative permeability response along the φ direction.

The negative refractive index of the constructed metamaterial has been proved by the prism experiment for transverse magnetic polarized incidence (Fig. 2b). The refractive index of the metamaterial is negative

from 8.1 to 9.5 GHz. The unit cell of the metamaterial has a size of 3 mm, which is less than one tenth of the wavelength at the negative refraction region of 31 to about 37 mm. The composite structure therefore can be considered as an effective homogenous left-handed medium. As long as the particle is traveling in the ρz plane, Cherenkov radiation phenomena in the proposed metamaterial is the same as those in isotropic left-handed metamaterial. (For a more in-depth analysis of the new metamaterial, see Box 1.)

With the presently available fabrication technology, it is possible to reach much higher frequencies by scaling down the corresponding metamaterial lengths. However, metals may no longer behave as perfect conductors at such frequencies, perhaps rendering them less effective for the purpose of building a left-handed material.

To choose the most suitable out of many possible metamaterial designs for reversed Cherenkov radiation, the following considerations need to be carefully studied:

- (1) The real parts of the components of $\mu_{\varphi\varphi}$, ϵ_{zz} , and $\epsilon_{\rho\rho}$ must be negative. Therefore the split-ring resonators and the metal wires should be in plane, i.e. they may be located in the same substrate layer or in the top or bottom sides of the layer. The coupling between them should be minimized. For example, the metal wires shown in Fig. 2a cross over the centre of the split-ring resonators without any contact. The total net magnetic flux perpendicular to

Box 1 Analyzing negativity

To see at what frequencies the new metamaterial in reference 34 is left-handed, consider the following. The effective permeability of the L-shaped split-ring resonators can be derived by computing the induced circumferential surface current per unit length J around the loop in a stack of rings, which behaves like a solenoid to an oscillating incident electromagnetic wave with a magnetic field H_0 polarized along the φ direction^{68,69}. Based on Ampere's law, the magnetic fields inside and outside of the loop are $H_{int} = H_0 + J - FJ$, and $H_{ext} = H_0 - FJ$, where F is the fractional area of the periodic unit cell in the pz plane occupied by the interior of the split-ring resonator. The average magnetic flux is $B_{ave} = \mu_0 F H_{int} + \mu_0 (1 - F) H_{ext}$ or $\mu_0 H_0$. This is expected since the B field due to the current loop is continuous, and so the net effect of the current on B_{ave} must vanish.

On the other hand, the net effect of the current on the average magnetic field density does not disappear. It is $H_{ave} = H_0 - M$, where $M = FJ$ is the magnetic dipole moment per unit volume of the material. The effective permeability is therefore $\mu_{eff} = B_{ave}/H_{ave} = \mu_0 H_0 / (H_0 - FJ)$. Using Faraday's law for electromagnetic force and letting the current in the metallic loop equal to the displacement current in the gap formed by the top and bottom L-strips yields the effective permeability of the split-ring resonators as a function of F , inductance, capacitance, and other geometrical and material parameters.

The resultant effective permeability follows a Lorentz dispersive model. For a perfect conductor, it is negative within the frequency range $\omega_0 \leq \omega \leq \omega_0 / [1 - FL_g / (L_g + L_i)]^{1/2}$, where L_g is the geometrical inductance and L_i the inertial inductance that arises from the finite electron mass in the metal. Using the parameters found in³⁴ yields $f_0 = (2\pi)^{-1} \omega_0 \approx 11$ GHz. Employing a computer method to accurately calculate the capacitance between the gap⁷⁰ by including the fringing electric effect, we get a more accurate resonant value around 8 GHz, in good agreement with the experimental results³⁴.

The magnetic response of the split-ring resonator to H_ρ and H_z fields is negligible, thus we get $\mu_{\rho\rho} = \mu_0$ and $\mu_{zz} = \mu_0$. The effective

magnetic parameters tensor of the structure is therefore given by $\mu = \text{diag}[\mu_{\parallel} \mu_{\perp} \mu_{\parallel}]$, where $\mu_{\perp} = \mu_{eff}$ following a Lorentz dispersive model, and $\mu_{\parallel} = \mu_0$.

The effective negative permittivity is determined by calculating the capacitances and inductances in the wire medium^{71,72,73}. These calculations show that the effective permittivity of the wire medium is negative below ω_{ep} , which is inversely related to the distance between two adjacent wires.

The electric response of the wire array follows a Drude dispersive model. The two-dimensional wire array shown in Fig. 2a behaves like an isotropic low frequency plasma in the xz plane. Since the electrical response of the wire medium to the E_y field can be neglected, the constitutive parameter tensor is therefore given by $\epsilon = \text{diag}[\epsilon_{\parallel} \epsilon_{\perp} \epsilon_{\parallel}]$, where $\epsilon_{\parallel} = \epsilon_{eff}$ following a Drude dispersive model, and $\epsilon_{\perp} = \epsilon_0$ is the dielectric constant of the background medium.

We can separate all field components into their φ , ρ , ζ components from the Maxwell equations²³. For the transverse magnetic case, the field depends on only the μ_{\perp} and ϵ_{\parallel} components. The original constitutive parameter tensors, which are 3x3 complex matrix, are therefore diagonalized here. The Maxwell equations are reduced to $k_s \times H_\varphi = -\omega \epsilon_{\parallel} E_s$, and $k_s \times E_s = \omega \mu_{\perp} H_\varphi$. Note that μ_{\perp} and ϵ_{\parallel} follow Lorentz and Drude dispersive model respectively. For the lossless case in the overlapped frequency band where both of them are negative, the time averaged Poynting vector is $\langle S \rangle = \langle E_s \times H_\varphi^* \rangle = k_s |E_s|^2 / (2\omega \mu_{\perp})$. This is opposite to the wave vector k_s for a negative μ_{\perp} representing a backward propagating wave. It also shows that E_s , H_φ , and k_s form a left-handed triad.

The Helmholtz wave equation gives $k_s = \frac{\omega n}{c}$, where the refractive index $n = \pm \sqrt{\frac{\mu_{\perp} \epsilon_{\parallel}}{\mu_0 \epsilon_0}}$. Since for any passive medium, analytic continuation arguments require the imaginary parts of the permeability, the permittivity, and the refractive index to be positive, we therefore must pick the negative sign for the solution of n .

the split-ring resonator plane produced by the induced currents in the wires vanishes due to the symmetry with respect to the wire, and therefore has little effect on the magnetic behavior of the split-ring resonator.

- (2) Since Cherenkov radiation is faint, a metamaterial with low loss is very important for successful detection. In the microwave frequencies, the dielectric loss dominates. Thus, a substrate with low loss should be used. At higher frequencies, such as in the terahertz or optical range, as mentioned above, a metal with a low loss such as silver or even superconductors may be needed. As dielectric loss is smaller compared with metallic loss at optical frequencies, some dielectric resonators with subwavelength resonant mode^{30,35} may also be used in metamaterial design for reversed Cherenkov radiation in those regions.

- (3) A metamaterial for reversed Cherenkov radiation must exhibit isotropic electrical response. The unit cell of the design therefore should have some kind of symmetry, such as rotational symmetry or rotoreflection symmetry.

Demonstrating reversed Cherenkov radiation

Even with the right metamaterial, it is challenging to experimentally test reversed Cherenkov radiation due to fabrication constraints. The intensity of Cherenkov radiation increases with higher frequencies, so the optical or ultraviolet spectrum is more suitable for detection. However, in order to create a metamaterial that is left-handed at optical or ultraviolet frequencies, the unit size of the metamaterial should be much smaller than the wavelength, which ranges from 700 to 10 nm. Although great effort has been devoted to push the working frequency of metamaterials from microwave to optical

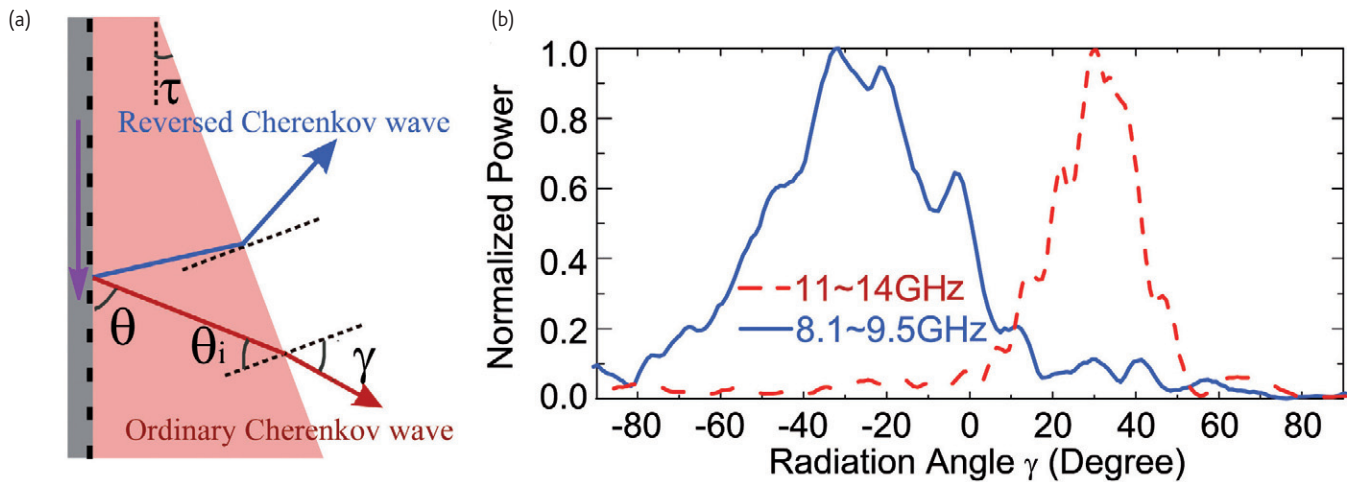


Fig. 3 (a) Experimental setup demonstrating reversed Cherenkov radiation, with a slot waveguide modeling a fast charged particle traveling from top to bottom (downward pointing purple arrow). The prism-like metamaterial filters the reversed Cherenkov wave, which is emitted backward from its origin and then refracted backward when exiting the left-handed metamaterial. (b) Sum of the radiation power in each angle in the negative refraction band (solid line) and positive refraction band (dashed line). Reprinted figure with permission from³⁴. © 2009 by the American Physical Society.

frequencies^{8,10,12,15-17,36-40}, fabrication techniques are still much less mature at optical frequencies. Furthermore, the loss in the metal increases as it scales to the optical spectrum, making the signal weaker and detection more difficult.

Another challenge involves measurement issues. Convincingly demonstrating reversed Cherenkov radiation in a left-handed medium requires measuring the far field of the radiated waves. However, it is not yet practical to build a large block of left-handed medium and measure the far field inside it.

Despite these challenges, Cherenkov radiation in a metamaterial-loaded waveguide with a charged particle beam incidence has been carried out at microwave frequencies⁴¹⁻⁴³. An energy peak in microwave radiation was observed at the left-handed band of the metamaterial, showing some evidence of Cherenkov radiation. Although backward Cherenkov radiation was not observed due to beam fluctuations⁴³, it was the first experimental attempt to use a charged particle beam to measure Cherenkov radiation in a metamaterial. In order to convincingly demonstrate the backward Cherenkov radiation in a left-handed medium, our group proposed the concept of using a waveguide with an array of open slots to emulate a fast moving charged particle. This setup sidesteps the problem of weak Cherenkov radiation from a charged particle in the microwave frequencies, enabling the verification of reversed Cherenkov radiation in the low frequency band³⁴.

To see why this is so, consider a monochromatic microwave propagating in the slot waveguide. As it does so, it is emitted through each of the slots with a fixed phase delay relative to its neighboring slots. This behavior occurs because the input microwaves take a longer time to travel to the more distant slots. The slot waveguide thus functions as a phased dipole array.

Comparing the electric current carried by a moving charged particle with the current density of the slot waveguide in the frequency

domain shows that they are very similar. One difference is that the moving charged particle contains the whole spectrum of frequencies. The slot waveguide, in contrast, has only one working frequency. As far as that single frequency is concerned, though, the radiation produced by moving charged particles and that by the phased dipole array are exactly the same. Therefore, the slot waveguide emulates a monochromatic Cherenkov source with its charged particle moving with a frequency-dependent speed of $v = \omega/k_z$.

In experiments, a prism-like sample is used for measurement instead of building a large block of left-handed medium. Although filled with air, the waveguide is directly in contact with the left-handed metamaterial and has an effective radius of about 5 mm. This distance is significantly smaller than the wavelength of interest which is larger than 30 mm. Consequently, the radiation is effectively emitted inside the left-handed metamaterial. During these experiments, the radiation is observed being emitted backward, as illustrated in Fig. 3. At the exit face of the left-handed metamaterial, the reversed Cherenkov wave gets further refracted into a negative refraction band while the ordinary Cherenkov wave gets refracted into a positive refraction band. Thus, the reversed Cherenkov wave can be easily distinguished from a forward Cherenkov wave (Fig. 3a).

An example using the parameters from these experiments directly demonstrates this backward emission of Cherenkov radiation. At 8.5 GHz, the real part of the index of refraction of the left-handed material is $n = -2.7$. The measured exit angle of the wave at the surface of the prism is $\gamma = -22^\circ$, therefore the incident angle of the radiation at the entrance of the prism is $\theta_i = 8^\circ$. The angle of the prism's exit surface is $\tau = 18.4^\circ$. Therefore, the emission angle from the source of $\theta = 90^\circ - \theta_i + \tau = 100.4^\circ$ is in the backward direction. This can be compared to the predicted value. Due to the phase difference between neighbouring slots in the experiment, the emission angle of the

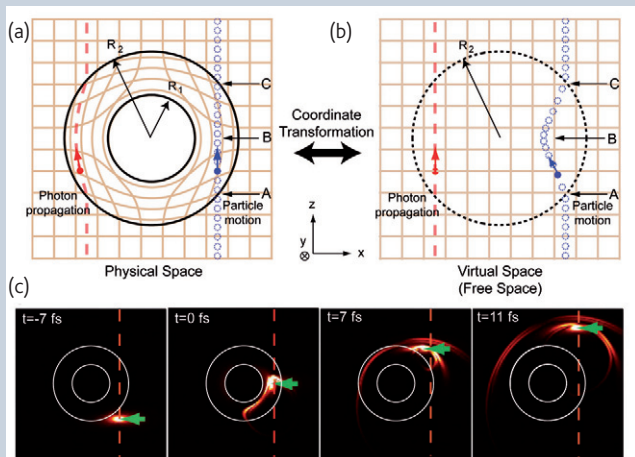
Box 2 Piercing invisibility cloaks

Theoretical work shows that the ideal cloak can be perfectly invisible from electromagnetic waves⁶¹. However, no matter in what frequency band the invisibility cloak works, it can still be electromagnetically detected. This could be done by shooting a fast charged beam through the cloak, which will not be refracted as the photons are⁵⁶.

With such a beam, a broadband Cherenkov wave would be radiated out as the particles travel through the cloak, making it visible. The characteristics of the photonic shockwave would not only reveal the cloak but would also provide information about its composition. This is because the angle of the emitted photons would depend upon the refractive index of the cloak.

A spherical invisibility cloak is a transformed curved electromagnetic space equivalent to a virtual flat electromagnetic free space for photons but not for a charged beam. Thus, Cherenkov radiation in the cloak can be viewed as a radiation phenomenon when a charged particle moves nonlinearly in a virtual curved space with a bent trajectory (Box 2 Fig. 1a and b). The velocity of the particle can be greater than the speed of light in the virtual electromagnetic space and thus generate radiation (Box 2 Fig. 1c).

In practice, this would require that the high-energy particle beam intersect the invisibility cloak. This could be done through some sort of scanning system. For practical reasons, this would probably be deployed at the entrance to a location. The beam, or multiple beams, would crisscross the opening, thereby ensuring that nothing unseen, or undetected, entered.



Box 2 Fig. 1 Trajectory of a fast-moving charged particle inside the transformation metamaterial-based cloak compared with the trajectory of a photon in (a) the physical curved electromagnetic space and (b) the virtual flat electromagnetic space. (c) E field of the Cherenkov wave radiated from a charged particle traveling through the curved electromagnetic space (here from a spherical cloak). Dotted line represents the trajectory of the particle beam with its centre marked with the small arrow. Reprinted figure with permission from⁵⁶. © 2009 by the American Physical Society.

radiation in vacuum from the slot waveguide is at 58° , equivalent to a particle speed of $1.9c$. In the left-handed metamaterial with $n = -2.7$, the corresponding backward emission angle of the radiation from the slot waveguide should then be 101.2° , which is in good agreement with the above measured value of 100.4° . The observed far field pattern in negative refraction band therefore demonstrates the reversed Cherenkov radiation in the left-handed medium (Fig. 3b).

Perspective and challenges

The unusual Cherenkov radiation in metamaterials opens a new window for many applications. For particle identification, reversed Cherenkov radiation has a distinct advantage: the photon and charged particle naturally separate in opposite directions so their physical interference is minimized.

Moreover, the left-handed metamaterial we have introduced is only electrically isotropic in two orthogonal directions. With further refinement, a metamaterial can be made to be isotropic, anisotropic, and bi-anisotropic. Many striking phenomena may be realized with such choices of materials⁴⁴⁻⁴⁸. One interesting possibility is that Cherenkov radiation without any velocity threshold may be generated by utilizing an anisotropic metamaterial. This unusual phenomenon has been previously observed in metallic grating⁴⁹ and photonic crystals^{50,51}. Here a metamaterial would provide an additional solution with more material flexibility. The radiation pattern would cover a much larger angle from forward to backward. Thus, a Cherenkov detector based on anisotropic metamaterial would possess strong velocity sensitivity and good radiation directionality.

Also, new phenomena are predicted to arise when fast particles travel in a layered medium⁵²⁻⁵⁶. An intriguing one is that electromagnetic detection of a perfect invisibility cloak becomes possible through the use of Cherenkov radiation⁵⁶. Such cloaks have received great interest recently⁵⁷⁻⁶⁷. Based on a transformation method, they rely on metamaterials with specific parameters to manipulate light. However, they cannot do the same for a particle beam and that provides a means to penetrate and detect them (See Box 2).


One way to look at backward Cherenkov radiation in the left-handed medium is as radiation phenomena arising from a charged particle moving in a virtual negative electromagnetic space. This concept opens up the door to even wider applications. By constructing the metamaterial with specific parameters to mimic the virtual electromagnetic space, we can flexibly manipulate the Cherenkov photons. These photons have potential applications in High Energy Physics, Astrophysics, and novel radiation sources.

As a first step, experimental work³⁴ has demonstrated that the manipulation of Cherenkov photon is possible in a left-handed medium. Future work will involve direct demonstration of reversed Cherenkov radiation using actual moving particles, which is crucial for practical applications. Achieving low loss metamaterials that work in

the optical spectrum is important as the sharp resonance easily allows the negative refractive index to be much smaller than -1 , the necessary condition to observe backward Cherenkov radiation. Another task is to develop three-dimensional optical metamaterials¹⁵⁻¹⁷, which are important to realize devices based on backward Cherenkov radiation.

Conclusion

Metamaterials, with their unusual electromagnetic properties, can enable many new applications, such as perfect lenses, invisibility cloaks, and reversed Cherenkov detectors. With the observation of backward emission, reversed Cherenkov radiation has been demonstrated and the corresponding detectors are now possible. With the transformation optics method, metamaterials with specific parameters could mimic

virtual electromagnetic space. This allows further control of the motion of the charged particle in the virtual space, offering great flexibility to manipulate the Cherenkov photons. The newly gained capability of flexible parameters may lead to further innovations in particle physics, astrophysics, and biomolecular science. 

Acknowledgements

We acknowledge the many useful manuscript comments and suggestions by Hank Hogan. Our research was supported by the Office of Naval Research under Contract No. N00014-06-1-0001, the Department of the Air Force under Contract No. FA8721-05-C-0002, the NNSFC (60801005,60990320, and 60990322), the FANEDD (200950), the ZJNSF (R1080320), and the Ph.D Programs Foundation of MEC (200803351025).

REFERENCES

1. Cerenkov, P. A., *Dokl Akad Nauk* (1934) **2**, 451.
2. Frank, I. M., and Tamm, I. E., *Compt Rend (Dokl)* (1937) **14**, 109.
3. Chamberlain, O., et al., *Phys Rev* (1955) **100**, 947.
4. Aubert, J. J., et al., *Phys Rev Lett* (1974) **33**, 1404.
5. Smith, D. R., et al., *Phys Rev Lett* (2000) **84**, 4184.
6. Shelby, R. A., et al., *Science* (2001) **292**, 77.
7. Smith, D. R., et al., *Science* (2004) **305**, 788.
8. Shalaev, V. M., *Nature Photon* (2007) **1**, 41.
9. Tsakmakidis, K. L., et al., *Nature* (2007) **450**, 397.
10. Soukoulis, C. M., et al., *Science* (2007) **315**, 47.
11. Smolyaninov, I. I., et al., *Science* (2007) **315**, 1699.
12. Lezec, H. J., et al., *Science* (2007) **316**, 430.
13. Engheta, N., *Science* (2007) **317**, 1698.
14. Hoffiman, A. J., et al., *Nature Mater* (2007) **6**, 946.
15. Yao, J., et al., *Science* (2008) **321**, 930.
16. Valentine, J., et al., *Nature* (2008) **455**, 376.
17. Liu N., et al., *Nature Mater* (2008) **7**, 31.
18. Genov, D. A., et al., *Nature Phys* (2009) **5**, 687.
19. Kundtz, N., and Smith, D. R., *Nature Mater* (2010) **9**, 129.
20. Chen, H. Y., et al., *Nature Mater* (2010) **9**, 387.
21. Veselago, V. G., *Sov Phys Usp* (1968) **10**, 509.
22. Jackson, J. D., *Classical Electrodynamics*, John Wiley and Sons, New York, (1999).
23. Kong, J. A., *Electromagnetic Wave Theory*, EMW Publishing, Cambridge, MA, (2005).
24. Minkowski, H., *Nachr Ges Wiss Gottingen* (1908) **53**. [Reprinted: *Math Ann* (1910) **68**, 472].
25. Lu, J., et al., *Opt Express* (2003) **11**, 723.
26. Musha, T., *Proceedings of the IEEE* (1972) **60**, 1475.
27. Kemp, B. A., et al., *Phys Rev A* (2007) **75**, 053810.
28. Shelby, R. A., et al., *Appl Phys Lett* (2001) **78**, 489.
29. Chen, H., et al., *Phys Rev E* (2004) **70**, 057605.
30. Peng, L., et al., *Phys Rev Lett* (2007) **98**, 157403.
31. Zhang, J., et al., *Appl Phys Lett* (2008) **92**, 084108.
32. Moser, H. O., et al., *Opt Express* (2009) **17**, 23914.
33. Wu, B. I., et al., *J Appl Phys* (2007) **102**, 114907.
34. Xi, S., et al., *Phys Rev Lett* (2009) **103**, 194801.
35. O'Brien, S., and Pendry, J. B., *J Phys: Condens Matter* (2002) **14**, 4035.
36. Shalaev, V. M., et al., *Opt Lett* (2005) **30**, 3356.
37. Zhang, S., et al., *Phys Rev Lett* (2005) **95**, 137404.
38. Zhang, S., et al., *J Opt Soc Am B* (2006) **23**, 434.
39. Dolling, G., et al., *Opt Lett* (2006) **31**, 1800.
40. Dolling G., et al., *Opt Lett* (2007) **32**, 53.
41. Antipov, S., et al., *Nucl Instrum Methods Phys Res A* (2007) **579**, 915.
42. Antipov, S., et al., *J Appl Phys* (2007) **102**, 034906.
43. Antipov, S., et al., *J Appl Phys* (2008) **104**, 014901.
44. Matloob, R., and Ghaffari, A., *Phys Rev A* (2004) **70**, 052116.
45. Cheng, M., *Opt Express* (2007) **15**, 9793.
46. Duan, Z. Y., et al., *J Appl Phys* (2008) **104**, 063303.
47. Duan, Z. Y., et al., *Opt Express* (2008) **16**, 18479.
48. Duan, Z. Y., et al., *J Phys D: Appl Phys* (2009) **42**, 185102.
49. Smith, S. J., and Purcell, E. M., *Phys Rev* (1953) **92**, 1069.
50. Luo, C., et al., *Science* (2003) **299**, 368.
51. Kremers, C., et al., *Phys Rev A* (2009) **79**, 013829.
52. Bliokh, Y. P., et al., *Phys Rev Lett* (2008) **100**, 244803.
53. Bakunov, M. I., et al., *Opt Express* (2010) **18**, 1684.
54. Galyamin, S. N., et al., *Phys Rev Lett* (2009) **19**, 194802.
55. Averkov, Y. O., and Yakovenko, V. M., *Phys Rev B* (2005) **72**, 205110.
56. Zhang, B., and Wu, B. I., *Phys Rev Lett* (2009) **103**, 243901.
57. Pendry, J. B., et al., *Science* (2006) **312**, 1780.
58. Leonhardt, U., *Science* (2006) **312**, 1777.
59. Schurig, D., et al., *Science* (2006) **314**, 977.
60. Cai, W. S., et al., *Nature Photon* (2007) **1**, 224.
61. Chen, H., et al., *Phys Rev Lett* (2007) **99**, 063903.
62. Shalaev, V. M., *Science* (2008) **322**, 384.
63. Liu, R., et al., *Science* (2009) **323**, 366.
64. Valentine, J., et al., *Nature Mater* (2009) **8**, 568.
65. Gabrielli, L. H., et al., *Nature Photon* (2009) **3**, 461.
66. Leonhardt, U., and Tyc, T., *Science* (2009) **323**, 110.
67. Ergin, T., et al., *Science* (2010) **328**, 337.
68. Pendry, J. B., et al., *IEEE Trans. Microwave Theory Tech* (1999) **47**, 2075.
69. O'Brien, S., and Pendry, J. B., *J Phys: Condens Matter* (2002) **14**, 6383.
70. Yuan, C. P., and Trick, T. N., *IEEE Electron Device Lett* (1982) **3**, 391.
71. Pendry, J. B., et al., *Phys Rev Lett* (1996) **76**, 4773.
72. Ramakrishna, S. A., *Rep Prog Phys* (2005) **68**, 449.
73. Ramakrishna, S. A., and Grzegorzczak, S. M., *Physics and Applications of Negative Refractive Index Materials*, CRC Press, (2009).